

# Reticulated PVA Foams: Preparation, Characterization and *in vitro* Evaluation for Potential 3D Microbiological Culture

R.V. Ferreira<sup>a</sup>, C. L. Cruz<sup>a</sup>, G. H. de Castro<sup>a</sup>, K. M. Freitas<sup>a</sup>, N. M. De Paula<sup>a</sup>, L. B. Nogueira<sup>a</sup>, C. S. B. Gil<sup>b</sup>,  
D.M. Freitas-Silva<sup>a\*</sup> 

<sup>a</sup>Centro Federal de Educação Tecnológica de Minas Gerais, Belo Horizonte, MG, Brasil

<sup>b</sup>Universidade Federal de Lavras, Lavras, MG, Brasil

Received: May 23, 2020; Revised: September 08, 2020; Accepted: October 15, 2020

The development of three-dimensional matrices for microbial cultures is a promising strategy by mimic the natural environments of cells and promoting adhesion, growth and cellular proliferation. In the current study, polyvinyl alcohol (PVA) foams were produced by the combination of gas foaming and freeze-drying for applied as microorganism 3D matrix. The spectra FTIR indicated consume of hydroxyl groups that evidences the crosslinking reaction and promoted increases in thermal stability. Morphological analysis by SEM revealed an interconnected porous structure in the PVA foams. Besides, the crosslinking reaction did not affect pore size and morphology. Meanwhile, cross-linked PVA foam (G-PVAFL) exhibited an increase of compressive modulus and compressive strength. The swelling ratio reached 85% and degradation kinetics of G-PVAFL showed a suitable profile to support microorganism in the biofilm formation. *Escherichia coli* (Gram-negative bacteria), *Staphylococcus aureus* (Gram-positive bacteria) and *Candida albicans* (yeast) were efficiently immobilized in G-PVAFL. In addition, cells morphology were preserved for all species investigated. Besides, Sugar Fermentation Test with *Escherichia coli* immobilized indicates the preservation of proliferative and metabolic activity. These results indicate that G-PVAFL is suitable as a matrix for 3D microbiological culture.

**Keywords:** Poly vinyl alcohol (PVA), crosslinking, microorganisms, 3D cell culture.

## 1. Introduction

Traditional strategies of microorganism growth have allowed drugs development and several applications in health, agriculture, industry and environment<sup>1</sup>. Microbial diversity represents an important source for the improvement of biology and biotechnology. Microorganism's growth on plane surfaces has advantages over growth in the liquid medium, like isolation and identification facility, study of different types of cells *in vitro*, drug screening and among others<sup>2</sup>. Although this model contributes to several advances in biological studies, it has limitations because cannot accurately simulate the rich environment and complex processes observed *in vivo*<sup>3</sup>.

In that perspective, three-dimensional matrices for the microorganism's growth can be an interesting approach. Despite the concept has been more explored for mammalian cell culture, some research has been published exploring the 3D bacterial culture<sup>4-6</sup>. Several methods have been used to develop 3D mammalian culture, as multicellular spheroids, organoids, organs-on-chips, 3D bioprinting and scaffolds, each with its advantages and disadvantages<sup>3,7</sup>.

Three-dimensional matrices for microorganism promote proliferation, increase biomass and metabolic activity<sup>8,9</sup> and mimic environmental conditions. Besides increase tolerance to inhibitors, temperature and pH variation; reduce production costs, as the same matrix can be used countless times without

significant loss of microbial activity<sup>10,11</sup>. 3D culture offers a structure that mimics cell behavior and organization *in vivo*, besides, ensures cell-cell communication and facilitates the control of cell growth monitoring<sup>12</sup>. Industrial application of 3D matrices incorporated with microorganisms includes in wastewater bioremediation<sup>13,14</sup> beer fermentation<sup>15</sup>, vinegar production<sup>16</sup> and soil fertilization<sup>17</sup>.

Other hand, microorganism's growth in 3D structures, that mimicking environmental conditions can develop biofilms, an aggregate of bacteria held together by a polysaccharide extracellular matrix<sup>18</sup>. Biofilms are advantageous to microorganism because they provide a nutrient-rich environment that facilitates growth and confer resistance to chemical agents like antibiotics. Therefore, in addition to industrial applications, the use of 3D matrices for microorganism's growth can also be a to study antimicrobial resistance<sup>5</sup>.

For a successful cell immobilization and proliferation, the pre-requisites of 3D matrices include the following: (i) three-dimensional interconnected porous structure to permit cell adhesion, growth, migration and efficient delivery of nutrients and oxygen to the cells; (ii) mechanical strength to provide support to the cells and maintain the three-dimensional structure and (iii) controllable biodegradation. The cultivation of multiple layers of 3D cells is possible by the development of porous and non-toxic matrices that provide good resistance, adhesion and greater contact surface<sup>19</sup>. Collagen<sup>20</sup>, polyurethane sponge<sup>21</sup>, poloxamer hydrogel<sup>22</sup>,

\*e-mail: [daniellemarra@cefetmg.br](mailto:daniellemarra@cefetmg.br)

porcine extracellular matrix<sup>23</sup>, polycarbonate membrane<sup>24</sup>, cellulose<sup>25</sup>, cellulose matrices on top of hydrogel<sup>26</sup>, hyaluronic acid and collagen scaffold<sup>27</sup> has been used as 3D matrices to grow microorganism.

Among the various biocompatible polymers used poly vinyl alcohol (PVA) present interesting features. PVA has been widely used to produce foam matrices for 3D cell culture and tissue regeneration due to combination biocompatibility, non-toxicity, easy to process and relative cheapness<sup>28</sup>. PVA foams provide excellent mechanical and pH stability, flexibility and the semi permeability allow transport of oxygen and nutrients that are necessary for cell survival as well as for the removal of wastes secreted by the cells<sup>29</sup>. Several techniques have been developed for the fabrication of PVA matrices that are able of providing an environment with interconnected pores for cell adhesion and proliferation. Conventional techniques including chemical gas foaming, solvent casting/particulate leaching and freeze-drying have been used to develop PVA matrices that can meet to 3D cell culture requirements. The method chemical foaming produces porous structures with pore size from 30 to 700  $\mu\text{m}$  and porosity up to 85%. However, it is difficult to ensure pore connectivity and control of the pore sizes space<sup>29,30</sup>. The matrix produced by solvent casting/particulate leaching has a high porosity from 50% to 90%, low cost and uses small amounts of polymer. However, the pore shape of foam produced by this method does not have controllable space. The freeze-drying method allows regulating the pore size by varying the freezing temperature and avoiding the use of toxic solvent. Nevertheless, the freeze-drying process should be controlled to prevent heterogeneity of the produced matrix<sup>29,30,31</sup>.

In addition, to improve mechanical properties and control the biodegradation rate in PVA foam, an important step in the processing of the material is crosslinking. This process increases the mechanical properties of the polymer; otherwise, the material does not have dimensional stability in the presence of water, which is necessary for its proper functioning. Glutaraldehyde has been the agent chosen for the formation of the cross-links, due to the ease of reacting with PVA chains, furthermore, it is known that this substance can be linked non-specifically to the biomolecules as the proteins and can be used to bind the PVA to these substances<sup>32</sup>.

The *in vitro* degradation behavior of a scaffold plays an important role in the success of 3D microorganism cell culture<sup>7,12,19,33</sup>. During the formation, deposition and organization of the microorganism cells, the scaffold must degrade while maintain a minimum mechanical resistance to support the new biofilm formation. The degradation process may involve several mechanisms that are related to the type and chemical composition of the material. For polymeric foam scaffolds, the main mechanisms of *in vitro* degradation involve dissolution or solvation in water, erosion, enzymatic cleavage, or hydrolytic chains in smaller molecules, among others<sup>33,34</sup>. The degradation affects the physical-chemical, morphological and mechanical properties of the scaffolds, therefore it is crucial to study the alterations in such properties, during the degradation process, to control the performance of the scaffold<sup>33</sup>.

In the present work, we have prepared cross-linked PVA foams and investigated the potential as 3D matrix for microorganism culture. The PVA foams were produced by a combination of conventional scaffold fabrication techniques gas foaming and freeze-drying. The material properties were evaluated by morphological, physicochemical, thermal and mechanical analysis. *In vitro* swelling and degradation tests were performed in order to evaluate the foam stability in microorganism cell culture conditions. Finally, the cross-linked PVA foams produced were used for the immobilization of *Escherichia coli* (Gram-negative bacteria), *Staphylococcus aureus* (Gram-positive bacteria) and *Candida albicans* (yeast) cells and the cell attachment and viability were evaluated.

## 2. Experimental

### 2.1 Materials

Polyvinyl alcohol (PVA, Mw ~ 145 000, hydrolysis rate >99%), glutaraldehyde (Mw = 100.12) and osmium tetroxide were purchased from Sigma-Aldrich. Calcium carbonate (CC), hydrochloric acid and sodium hydroxide were purchased from VETEC. Acetone was purchased from Anidrol. Mueller-Hinton agar and nutrient broth were purchased from Kasvi, (Italia). All chemical compounds were used as received.

### 2.2 Preparation of PVA foams

PVA foams were produced by the combination of chemical gas foaming with 33% m/m of PVA/foaming agent followed by freeze-drying methods and it cross-linked with 1% of glutaraldehyde. Sample preparation was performed followed the studies conducted by Bai et al.<sup>18</sup>. PVA foam was prepared as it follows: PVA (15% m/v) was added to distilled water containing calcium carbonate (PVA/CC 2:1) by a mechanical stirrer in a boiling water bath at temperatures of  $80 \pm 5$  °C, for 2 h. After the complete solubilization, the mixture was cooled to room temperature, hydrochloric acid (5 M) was gently added and the mixture was stirred vigorously to produce gas bubbles. Thereafter, the PVA foam was frozen at -18 °C. The final PVA/GA molar ratio was 0.07. After 48 hours the foam was thawed at room temperature, submerged in NaOH (1 M) containing 1.0% of glutaraldehyde and stirred gently at 35 °C for 2 h. After the cross-linking step, the samples were washed with distilled water until they reach pH 7. The samples were washed in distilled water to remove non-leached salt. Finally, in the last step, the samples were placed on a polypropylene becker (10 mL), frozen in liquid nitrogen and freeze-dried (Terroni TL-600). This sample was named G-PVAFL. The sample PVAFL was obtained by a similar procedure described, without crosslinking with the glutaraldehyde.

### 2.3 Physicochemical characterization of PVA foams

The PVA foams were evaluated by Fourier Transform Infrared Spectroscopy (FTIR) Shimadzu, model IRPrestige-21, in the range between 4000 and 400  $\text{cm}^{-1}$ . Thermal analysis of the foams was done by differential scanning calorimetry (DSC) using a DSC Q2000 instrument (TA Instruments), in

N<sub>2</sub> atmosphere of 50 mL/min. The heating scan was done from 30 to 300 °C at 10 °C/min. The melting enthalpy ( $\Delta H_m$ ) obtained from the melting peak area was used to estimate the crystallinity ( $X_c$ ) of the samples using the following Equation 1:

$$X_c = \Delta H_m / \Delta H^* \quad (1)$$

Where  $\Delta H^*$  is the melting enthalpy for 100% crystalline PVA<sup>35</sup>.

The morphological characterization of the PVA foams was investigated by scanning electron microscopy (SEM) using Shimadzu model SSX-500 equipment. The PVA foam samples were frozen in liquid nitrogen and fractured using a scalpel. Then, samples were sputter-coated with gold to a thickness of 200–500 Å and positioned on a metal stub for observation under SEM. Compressive testing was conducted by ASTM standards D695-02. The test was conducted on three samples of PVA foams cylindrical specimens with 12 mm diameter and 24 mm height. Testing was performed using the universal testing machine Shimadzu AG-X in compression mode at a speed of 10 mm/min and the specimens were compressed to 50% strain, with 10 kN loading. The normal force was recorded and used to calculate the compressive modulus for each sample. The initial diameter and area of each sample were measured and recorded before testing. The compressive modulus was calculated as the slope of the initial linear portion of the stress-strain curve.

The swelling kinetics was estimated at room temperature with a gravimetric measurement as previously described by<sup>36</sup>. The initial dry mass ( $d$ ) of the foams was measured and then was placed in distilled water. The wet weight ( $w$ ) was measured for 18 minutes, every 2 minutes and then it was carried out again after 24 hours. The experiment was performed in triplicate. The swelling percentage was calculated with the following Equation 2:

$$SR\% = [(w - d) / d] \times 100\% \quad (2)$$

The *in vitro* degradation tests were performed according to the methodology described by Courtney et al.<sup>7</sup>. The samples were soaked in 3 mL of PBS (phosphate saline buffer) at 37 °C. The weights of the PVA foams were measured after 1, 3, 7, 14, 21 and 30 days. PVA foam degradation was evaluated in terms of weight loss, morphological variations and mechanical properties concerning the immersion time. The measured mass for the sample none degraded ( $M_{si}$ ) and for the samples incubated in different time intervals ( $M_{sf}$ ) were used to compute the mass variation according to the Equation 3:

$$\Delta M = \frac{M_{si} - M_{sf}}{M_{si}} \times 100\% \quad (3)$$

## 2.4 Microorganisms assays

The cross-linked PVA foams were subjected to different gamma-irradiation doses (2, 10, 15 and 20 KGy). To verify the sterility of such doses, the direct inoculation test of PVA foam in Mueller-Hinton agar plates was performed. Samples were analyzed for microorganism growth at 24, 48 and 72 h after the incubation.

The strains of clinical relevance were grown in nutrient broth. *Escherichia coli* (ATCC 25922), *Staphylococcus aureus* (ATCC 6538) were used as gram-negative and gram-positive bacteria models, respectively in broth at pH 7. *Candida albicans* (ATCC 10239) was grown at pH 5 and used as a yeast model. The cells were harvested at the end of the exponential growth phase. Ten  $\mu$ L of inoculum were into nutrient agar and incubated at 37 °C and 28 °C for 24 h, for bacterial and yeast, respectively. Three single colonies were randomly selected and inoculated into 10 mL of nutrient broth. Subsequently, 1 mL of microbial inoculum was transferred to a conical flask containing 3 x 3 mm sterilized cross-linked PVA foam and stirred.

After 15 min and/or 18 h of incubation, came up, then the foams were carefully removed and submitted to the fixing process. The foams were rinsed with PBS and fixed overnight in 1% osmium tetroxide, then it was dehydrated by sequential immersions in increasing concentrations of acetone (50%, 70%, 80% and 90%, w/v) and twice in anhydrous acetone and finally dried. The samples were bathed in liquid nitrogen and subsequently cut with a sterile scalpel, coated with gold and examined by SEM.

A Sugar fermentation test was carried out to verify the maintenance of biochemical activity of the microorganisms immobilized in cross-linked PVA foams. The indicator sugar of the broth was prepared using nutrient broth containing fermentable sugar (lactose, 20g/L). About ten milliliters of sugar broth was poured into each of the Durham tubes. Sterilized foams were incubated for 15 minutes in nutrient broth containing approximately  $2 \times 10^8$  *E. coli* cells (0.5 McFarland scale) at 28 °C. After the foams were carefully removed, washed with PBS and transferred to tubes containing lactose supplemented nutrient broth. Next incubation for 18 h at 28 °C, the presence of bacteria was analyzed by turbidity of the broth and gas production was indicated by displacement of the medium in the Durham tubes<sup>38</sup>.

## 2.5 Statistical analysis

All the experiments were performed in triplicate. The graphics were made using the GraphPad Prism software (Version 5.0®, San Diego, USA). Results are expressed as the mean  $\pm$  standard error (SEM). T-student test was applied to assess the statistical significance of differences; statistic confidence was 95% ( $p < 0.05$ ). The average diameter of 200 porous and the diameter distribution in the PVA foams was measured using IMAGE J software.

## 3. Results and Discussion

### 3.1. Physicochemical characterization of PVA foams

In order to evaluate the efficacy of the cross-linking reaction (Figure 1a), FTIR spectra was obtained. Figure 1b shows the spectra of PVAFL and G-PVAFL. The foams exhibit all major peaks related to hydroxyl and alkyl groups.

The spectra of the PVAFL and G-PVAFL exhibited characteristic absorption peaks at 1146  $\text{cm}^{-1}$ , 1190  $\text{cm}^{-1}$  and 842  $\text{cm}^{-1}$  which can be attributed to stretching vibration of C–O from the C–O–C and the stretching of C–O from the C–O–H bridge of PVA molecule. For the G-PVAFL foam, it

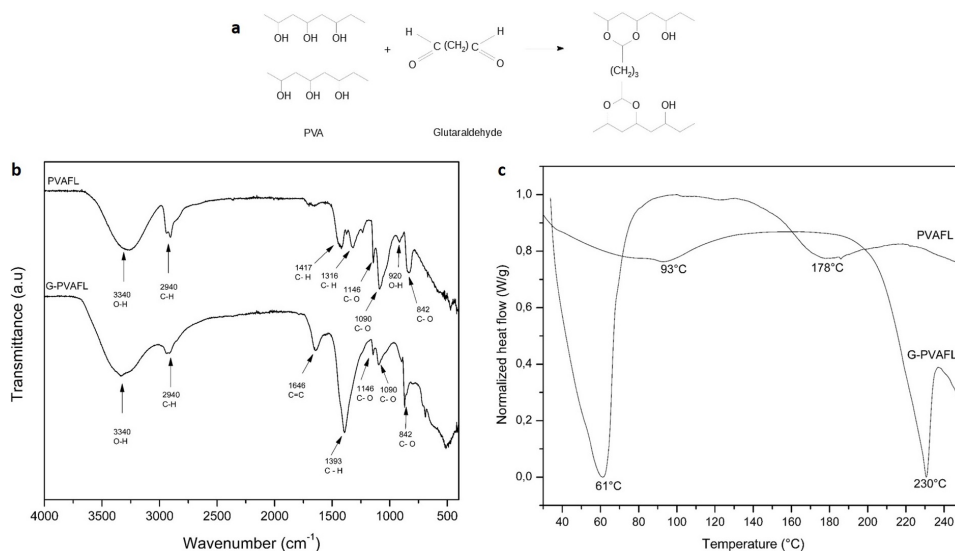


**Figure 1.** a. Cross-linking reaction with glutaraldehyde; b. FTIR spectra of PVAFL and G-PVAFL; c. DSC curves of PVAFL and G-PVAFL.

is possible to observe the reduction of the relative intensity of the C-O bands related to the alcohol groups. Such results evidence that the cross-linking reaction took place consuming hydroxyl groups. In addition, the peak at 1650 cm<sup>-1</sup> attributed to C=C was observed in the G-PVAFL sample, indicating some degradation of the polymer in the reaction conditions<sup>17</sup>. The glutaraldehyde molecule exhibits characteristic bands at 2850-2750 cm<sup>-1</sup> and 1720-1740 cm<sup>-1</sup> related to C-H and C=O stretching, respectively. According to the spectra obtained for the G-PVAFL sample, these peaks are absent indicating complete reaction of the glutaraldehyde with the OH groups from PVA during the cross-linked network formation<sup>17,39</sup>.

DSC thermograms were used to determine glass transition temperature ( $T_g$ ) and melting temperature ( $T_m$ ) of the PVAFL and G-PVAFL samples (Figure 1c).

PVAFL and G-PVAFL foams yielded a  $T_g$  of 61°C and 93°C, respectively. An increase in melting temperature was also observed for G-PVAFL samples ( $T_m = 230°C$ ) compared to PVAFL samples ( $T_m = 178°C$ ). These results are indicators that the samples were cross-linked leading to  $T_g$  and  $T_m$  increasing due to reduced mobility of the polymer chains. Similar results were obtained in previous works<sup>17,40</sup>.

The melting enthalpy obtained for PVAFL and G-PVAFL were 21.5 J/g and 69.9 J/g, respectively, which are in agreement with previous works that produced PVA scaffolds<sup>41,42,43</sup>. The degree of crystallinity, obtained by Equation 1, was 15.5% and 50.4% for PVAFL and G-PVAFL, respectively. The enhancement of crystallization due to crosslinking was shown in previous work for PVA with high molecular weight (88,000 – 114,000 g/mol)<sup>44</sup>. According to Ma et al.<sup>4</sup> this behavior can be attributed to the self-nucleation effect related to the crosslinking sites in the PVA molecules, which is more significant for higher molecular weight polymer.

The SEM images (Figure 2) exhibit the PVAFL and G-PVAFL morphology. The images reveal that both foams have shown similar morphology. The samples exhibited an irregular porous structure, with an average diameter of 208 ± 176 μm and 277 ± 205 μm for PVAFL and G-PVAFL, respectively. The evidence of porous interconnectivity could

be observed for both samples. The histogram obtained for the samples (Figure 2c and 2d) shows a broad porous size distribution with size ranged from 22 to 937 μm and 35 to 977 μm for PVAFL and G-PVAFL, respectively.

In addition, the distribution size analysis reveals that 90% of pores in the foams had a diameter smaller than 460 μm. The pores with the lower average size can be associated with the freeze-drying process. Although, the larger porous were produced the CO<sub>2</sub> bubbles released by the chemical reaction between the calcium carbonate and hydrochloric acid during the gas foaming process. Dattola et al.<sup>6</sup> showed similar results with PVA foam fabricated by a combination of gas foaming and freeze-drying method. Therefore, the results indicate that crosslinking reaction with glutaraldehyde did not affect pore size distribution and pore morphology. These findings are in agreement with previous work, which showed the macro porous network was comparable between PVA foams with or without crosslinking with glutaraldehyde<sup>45</sup>.

The foam morphology exhibited by the samples is adequate for the microorganism's adhesion and proliferation. For a successful biocolonization, it is crucial that the isolated cells adhere in the foam surface and access the foam interior through the interconnected pores. In addition, the highly interconnected pores permit that nutrients and oxygen are delivered to cells located in the foam interior.

The influence of crosslinking on the mechanical properties of PVA was investigated by a compression test (Figure 3a). The non-crosslinking PVA foams (PVAFL) had poor mechanical properties with compressive modulus and compressive strength of 3.0 ± 0.2 KPa and 1.5 ± 0.1 KPa, respectively. These results are in agreement with Ye et al.<sup>6</sup> that investigated the mechanical properties of PVA foam obtaining compressive modulus values ranging from 2.0 to 11.0 KPa. As expected, crosslinking significantly improved the mechanical strength of the PVA foam resulting in an increase in compressive modulus (690 ± 5 KPa) and compressive strength (345 ± 5 KPa). Crosslinking creates anchor points between the PVA chains, which reduces the mobility of PVA units increasing stiffness and mechanical strength<sup>47,48</sup>.

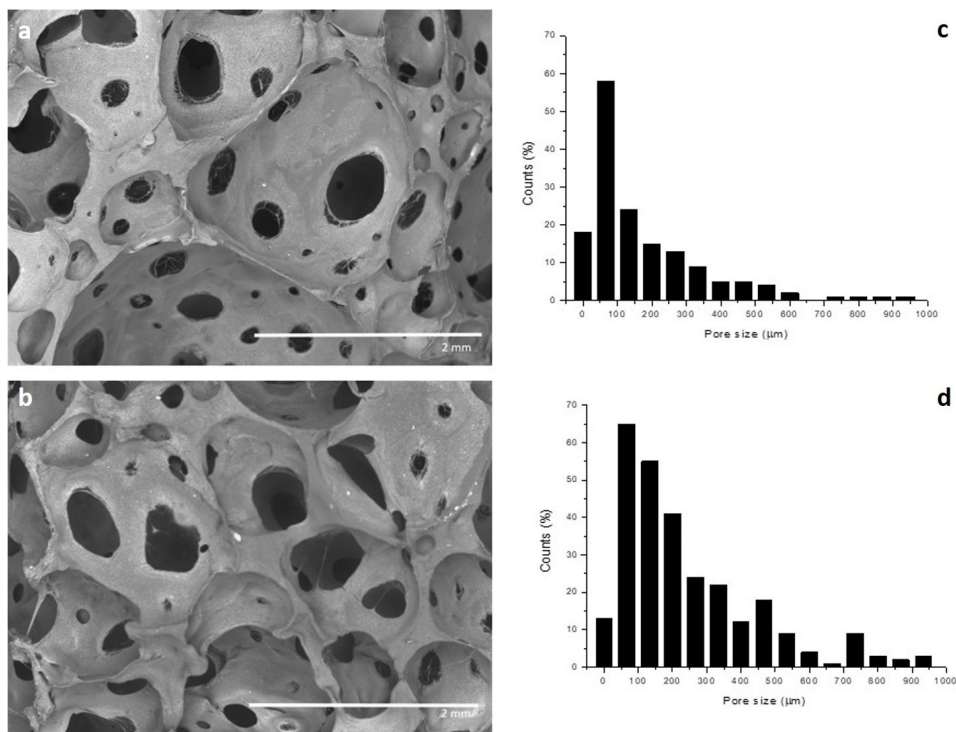


**Figure 2.** SEM images of PVAFL (a) and G-PVAFL foams (b) and size distribution of PVAFL (c) and G-PVAFL (d).

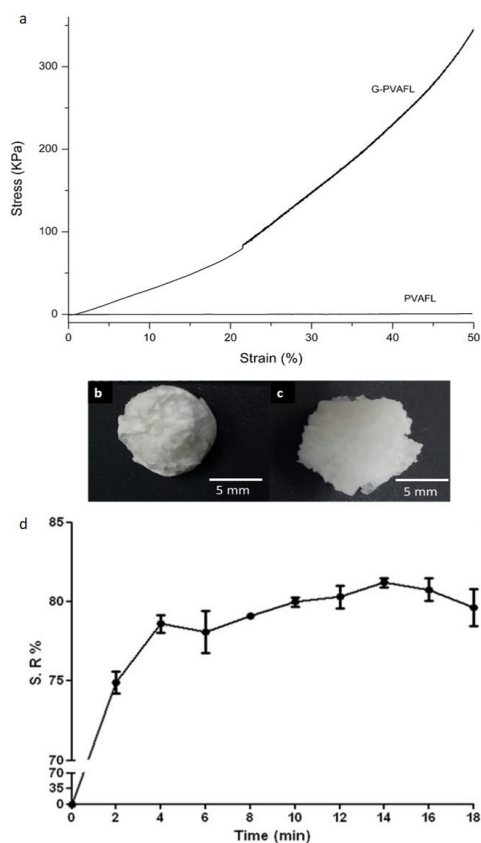


**Figure 3.** a. Stress-strain compression curves obtained for PVAFL and G-PVAFL; b-d. Macroscopic view in dry (b) and after 24 hours of water uptake (c) conditions of G-PVAFL. (d) Swelling rate of G-PVAFL.

**Table 1.** Physicochemical characterization of PVA foams.

	PVAFL	G-PVAFL
FTIR Peaks (cm <sup>-1</sup> )	1146, 1090, 842	1146, 1090, 842*
T <sub>g</sub> (°C)	61	93
T <sub>m</sub> (°C)	178	230
Average Pore diameter (μm)	208 ± 176	277 ± 205
Compressive strength (KPa)	1.5 ± 0.1	345 ± 5
Compressive modulus (KPa)	3.0 ± 0.2	690 ± 5

\* Reduction of the relative intensity compared to PVAFL.

G-PVAFL exhibited compressive modulus and strength values are lower than the values obtained for PVA cross-linked with glutaraldehyde in the previous work<sup>49</sup>. This behavior can be attributed to the presence of porous in the scaffold structure. According to Fan et al.<sup>50</sup> mechanical properties are reduced appreciably by the introduction of porosity. Several previous published studies showed a decrease in mechanical properties due to the enhancement of porosity<sup>46,51-54</sup>.

The results obtained in the physicochemical characterization assays of PVA foams were showed in Table 1.

After the crosslink reaction, there is a decrease in the intensity of the main FTIR peaks and an increase in T<sub>g</sub>, T<sub>m</sub>, compressive strength and compressive modulus. Nevertheless, there is not a significant changed in average pore diameter. Besides, the PVAFL showed poor stability and low mechanical stability in aqueous medium, which promotes damage in the integrity of the foam during the manipulation for swelling and degradation studies. Due to this behavior, the following experiments were performed only with cross-linked PVA foam. The water uptake was determined for G-PVAFL *in*

*vitro* in a period of 20 minutes and 24 hours. The water absorption study is shown in Figure 3b-d.

The G-PVAFL foam absorbed an amount of water 8 times greater, in 24 hours, compared to the dry weight maintaining the three-dimensional structure, as showed in Figure 3b and 3c. The foam swelled up to 75% of its original weight in 2 min, and reached the equilibrium in 4 min with 80% weight increased. As shown in Figure 3d, the water uptake in PVA foams rapidly increased and established an equilibrium after 4 minutes, keeping approximately the same weight until 18 minutes. After 24 hours, the weight increase reached 85%, with no appreciable changes in the foam structure. This swelling rate is low weather compared to the expected index for non-cross-linked PVA. However, the low degree of swelling obtained for GPVAFL is in agreement with previous studies. Morandim-Giannetti et al.<sup>5</sup>, showed that the addition of glutaraldehyde as crosslinking agent promoted a decrease of polymer water uptake. The crosslink density affects the swelling ratio due to the hydroxyls group consume of the PVA molecule. The glutaraldehyde molecule reacts with hydroxyl groups to form acetals, which produce a polymer less capable of hydrogen bonding with water molecules. In addition, the cross-linked polymer has smaller intermolecular spaces, which difficult the water molecule absorption.

The G-PVAFL degradation in similar conditions to the microorganism's cell culture was evaluated by measurements of weight loss, compressive modulus and SEM microscopy during 30 days. Figure 4a shows the weight loss of G-PVAFL during the *in vitro* degradation test. The weight loss was not significant until the 3<sup>rd</sup> day (4%). On the 7<sup>th</sup> day, an expressive weight loss could be observed (13%). The weight loss increased gradually reaching 57% at the 30 day.

The compressive modulus was examined during the degradation test (Figure 4b). Initially, G-PVAFL showed a compressive modulus of  $690 \pm 5$  KPa. The compressive modulus decrease gradually, reaching  $280 \pm 4$  KPa on the 7<sup>th</sup> day, i.e., a reduction of 60% compared to the initial value. After the 14<sup>th</sup> day, the foam exhibited a progressive increase, which can be attributed to the pore closure process, as showed in the SEM image (Figure 4c-h). Finally, after 30 days of incubation, the foam sample exhibited another drop-off to  $287 \pm 2$  kPa, which can be attributed to polymer degradation.

SEM was used to examine the foam morphology during degradation (Figure 4c-h). Figures 4c and 4d reveal that after three days the sample maintained the surface morphology observed for the sample not submitted to the degradation test. The porous interconnectivity was not affected and the porous maintained the morphology. After 7 days, it was possible to observe small changes in the porous size range. The diameter range obtained for this sample was 111-1676  $\mu\text{m}$ . However, the surface of the G-PVAFL sample maintained an appreciable amount of porous interconnected. On the 14<sup>th</sup> day, it was possible to observe a significant decrease in porous. After 21 days, the porous disappear and the foam surface exhibits cracks as a result of the shrunken pores. Finally, at 30 days, the foam presented a rough surface, with some cracks.

Several mechanisms can be involved in the *in vitro* degradation of polymeric scaffolds as dissolution solvation

in the aqueous, erosion, hydrolytic cleavage, among others<sup>34</sup>. Previous work has shown that the degradation of cross-linked PVA can be described as a combination of solvation and degradation/bulk erosion<sup>45</sup>. A similar degradation mechanism is proposed for the G-PVAFL foam occurring in three main stages.

The first stage (from day 1 until day 7) exhibited progressively mass and compressive modulus decrease. No significant changes could be observed in the porosity and pore morphology until the 7<sup>th</sup> day. This stage can be described as swelling and solvation of the polymer<sup>55</sup>. The next stage (between 14 and 21 days) presents significant changes in the polymer morphology with a reduction of porosity expressive mass loss and an increase of polymer compressive modulus. These findings can be associated with swelling or solvation of the polymer. The aqueous media diffuses into the foam which turns into a gradually swollen structure with closed porous. In this stage, it is expected that the effect of PVA as a water-soluble hydrophilic polymer will be most predominant. The increase in the compressive modulus value can be attributed to the porous closure<sup>34,45</sup>. In the last stage, day 30, hydrolytic reactions may occur, producing some polymer fragments and small molecules, which may diffuse outwards, increasing the mass loss. At this point, relevant erosion may dominate conducting to a considerable reduction of the mass and compressive modulus.

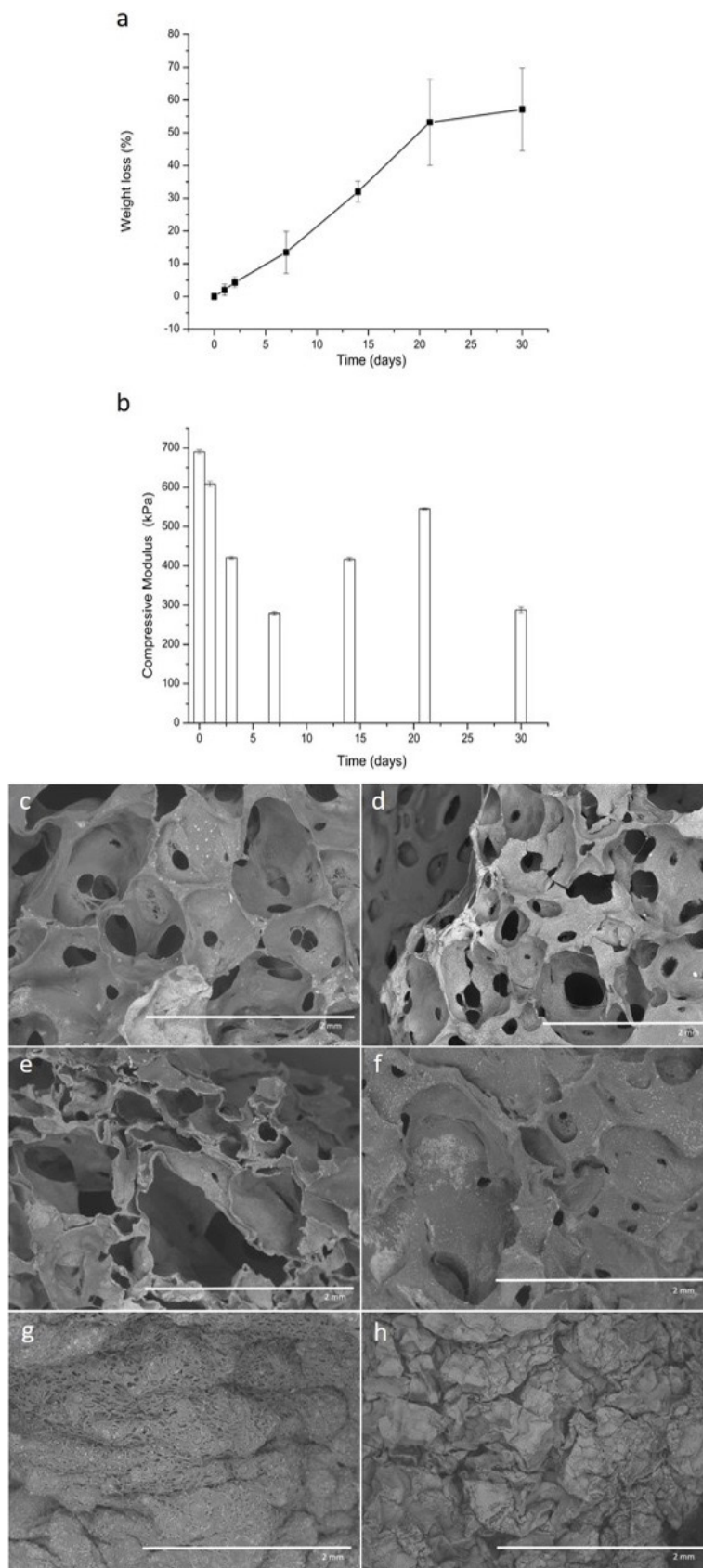
One important function of the 3D matrices is the appropriate degradation properties, which have to fit the rate of biofilm formation that would need around 14 days to be completed. According to Ning et al.<sup>5</sup> the mature biofilm is obtained between 5 and 14 days of microorganism culture in a scaffold. On the first day, free-swimming bacteria attach to the scaffold surface. Between day 1 and 2 bacteria aggregate forming microcolonies followed by progressive secretion of polysaccharides, proteins and oligonucleotides, which form a biofilm extracellular matrix and mature biofilm from day 5 to day 14. The last step consists of the spontaneous release of microbial cells into the surrounding culture media, which take place between 23 and 28 days.

In the current study, G-PVAFL was produced followed the previously methodology described by Bai et al.<sup>17</sup>. However, for the first time, the degradation kinetics is proposed into account mechanical strength and porosity of the polymer. Additionally, this kinetics shows suitable performance to support microorganism the biofilm formation. Given these results, the G-PVAFL has named PVA matrix and subjected to biological characterization using *Escherichia coli*, *Staphylococcus aureus* and *Candida albicans*.

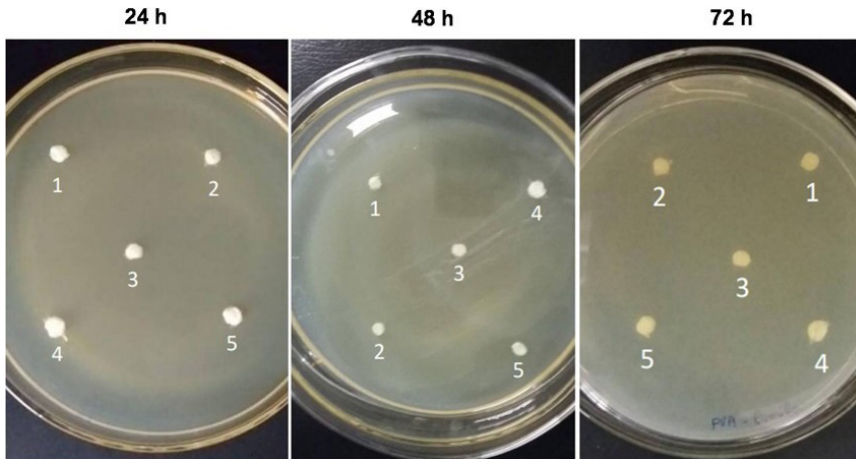
### 3.2. Microorganisms assay

Figure 5 shows PVA matrices absence of microbial growth at all radiation doses and analyzed times.

Thus, the sterilization method was effective even at low doses of 2 kGy. Non-sterile PVA foam has not shown in microorganism's growth in direct contact with agar, however, different studies show that pure PVA foam does not have any antibacterial action<sup>56, 57</sup>. The results suggest that the method employed, in the present study, may not be satisfactory to verify the presence or absence of microorganisms in non-sterile material. Thus, to ensure



**Figure 4.** **a.** Degradation test of G-PVAFL; **b.** G-PVAFL compressive modulus as a function of the degradation time; **c-h.** SEM micrographs of polymers at various time points of degradation (c) 1 day; (d) 3 days; (e) 7 days; (f) 14 days; (g) 21 days and (h) 30 days.



**Figure 5.** Evaluation of sterilization on irradiated PVA matrices. (1) non-sterile and sterile matrices with different doses of gamma radiation (2) 2 kGy, (3) 10 kGy, (4) 15 kGy and (5) 20 kGy.

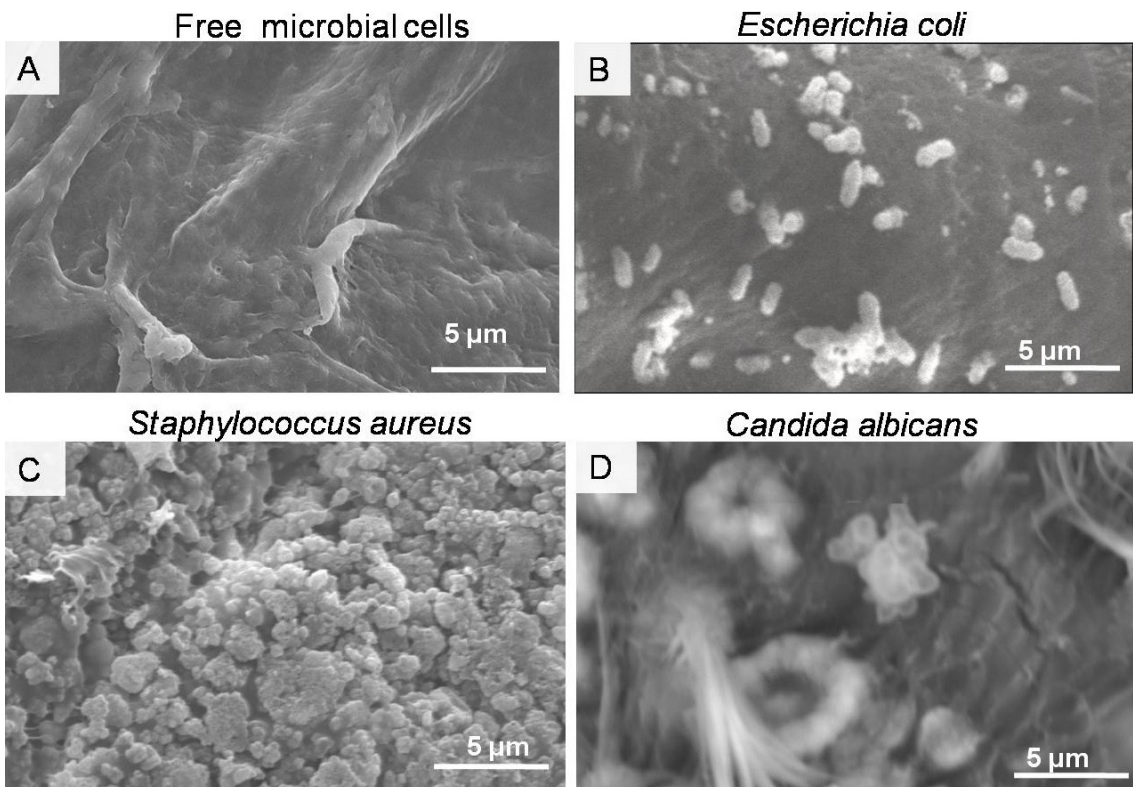


**Figure 6.** Microbial cells immobilized in PVA matrices. The images shows the presence of bacteria *E.coli* (b), *S.aureus* (c) and *C. albicans* (d) and absence (a).

no interference in microorganism's immobilization assay, the foams that received the 10 kGy irradiation dose were chosen. Studies conducted by Sasaki et al.<sup>8</sup> suggest that the irradiation treatment by gamma ray at 5 kGy or 10 kGy is expected to be optimal. Furthermore, the gamma irradiation did not change the FTIR spectra of cross-linked PVA foams (data not shown), suggesting that this sterilization method did not modify the PVA chain.

The PVA matrices were tested for adhesion cellular after soaking in a microbial culture suspension and observed

using SEM. Figure 6 shows the images captured by SEM after contact with bacteria *E. coli* (Figure 6b), *S. aureus* (Figure 6c) and fungus *C. albicans* (Figure 6d) are presented. We observed the colonization of microorganisms on the foam surface, besides distinguishing the morphology of type of microbial population. The PVA matrices immersed in suspension with *E. coli* strain morphologically present cells non-spore-forming, straight rod arranged in pairs or singly and those in contact with *S. aureus* shown higher density of cells in coccus-shaped and generally occur in grape-like

clusters. The matrices in contact with fungi have diploid and pseudohyphal and hyphal filaments cells (elongated cells).

In all PVA matrices in contact with the microorganisms were identified cells both on the surface and inside (not shown) the material. According to Oh et al.<sup>59</sup> the interaction between the material and the microorganism is due to the adhesive forces through van der Waals and electrostatic double-layer interactions, besides, it suggests the influence of factors such as hydrophobicity and decreased surface energy of the support for the success of this interaction. In this study, this colonization suggests that the porosity and interconnectivity of PVA matrices contribute to diffusion of microorganisms and nutrients<sup>17</sup>.

Three-dimensional cell culture models are considered to be a more functional replacement and are strongly applied as infection models for the study of motility and morphology of eukaryotes cells infected by microorganisms<sup>60,61</sup>, eg *Toxoplasma gondii*<sup>62,63</sup>. Studies conducted by Danielson et al.<sup>64</sup> compared the cultivation of the *T. gondii* between 2D and 3D culture and both systems reproduce similar conditions parasitic replication; however, layered culture favors the morphology and organization of the parasite mimetizing *in vivo* conditions.

After proving the efficiency of the immobilization of microorganisms in the foam, we analyzed the biomaterial's ability to adsorb suspended microorganisms. For this purpose, a short incubation period of 15 min to *E. coli* was determined, corresponding to a period prior to exponential growth - bacterial life cycle<sup>65</sup>. Figure 7b shows inside of PVA matrix, this structure offered favorable conditions for the microorganisms adhesion, also, it enables the viability and growth of adhered microorganisms as shown in Figure 7c (tube 3) by turbidity of the medium after incubation at

37 °C for 18 h, which confirms the presence of viable bacteria. These data suggest the physiology preservation of immobilized microorganisms and reflect the effectiveness of cell migration between the PVA matrix pores.

Therefore, a porous matrix with adequate morphology must guarantee an efficient mass transfer by diffusion of any substance (nutrient, oxygen, among others) and consequently successful colonization of microorganisms<sup>66</sup>. To evaluate the proliferation of microorganisms within the matrix structure, after an incubation period of 15 min to *E. coli*, the foams were washed 4-fold in PBS solution, transferred to another tube with nutrient broth and incubated. Figure 8b shows that PVA foam favors cell adhesion and provides favorable conditions for proliferation. Cell viability of microorganism after PVA matrix colonization was investigated. Figure 8c shows tubes containing immobilized cells presented a cloudy medium with precipitated indicative of viability and cell growth. In addition, it was possible to evaluate bacterial metabolism by visualizing a gas bubble in a Durham tube strongly suggesting that immobilization not only preserves the proliferative capacity of bacteria but also metabolic activity.

Our studies have shown that cross-linked PVA foam is suitable for use as a matrix for 3D microorganism culture. The data suggest that the polymeric matrix produced in the present work is easily colonized by different microorganisms with considerable microbial cell density and can progress to formation of the extracellular matrix and form a mature 3D biofilm structure. *E. coli* is a strain widely studied for being a common host for biotechnological applications due to its easy genetic manipulation and protein expression<sup>66</sup>. PVA matrix biocolonization by *S. aureus* and *C. albicans* (Figure 6) suggests that these microorganisms maintain their

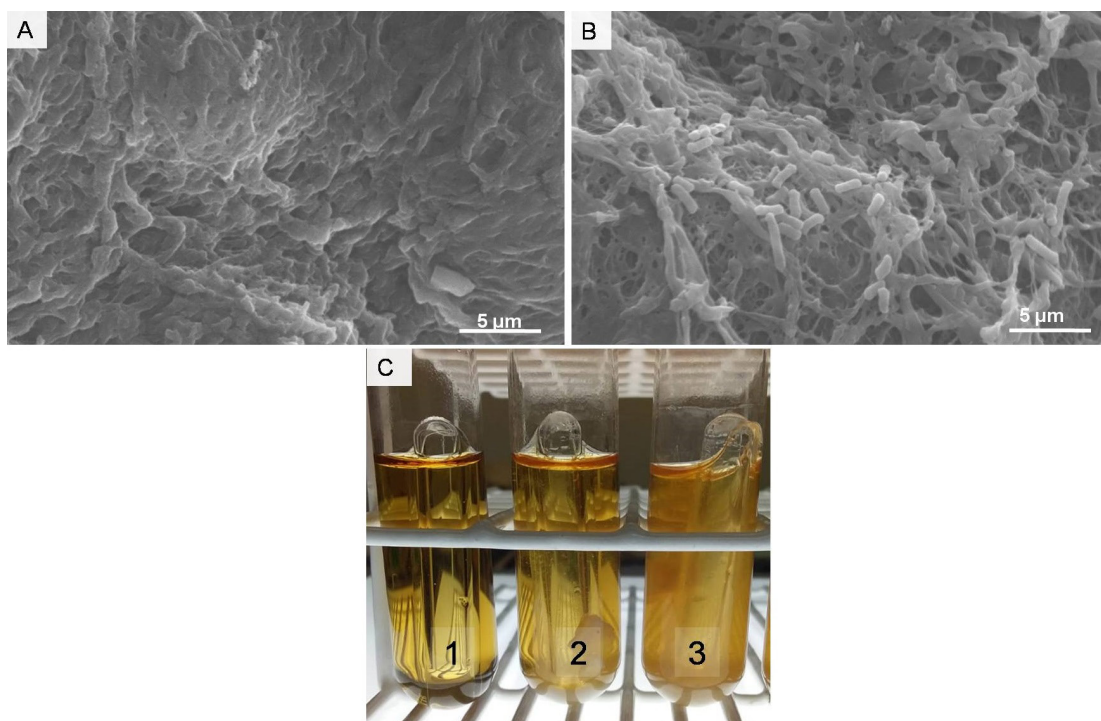


**Figure 7.** Microbial adhesion in PVA matrices and cell activity in lactose broth. The images shows foam with absence (a) and presence of bacteria *E. coli* (b) and (c) Durham tube assay: tube 1- blank; tube 2- foam alone; tube 3- foam + microorganism.

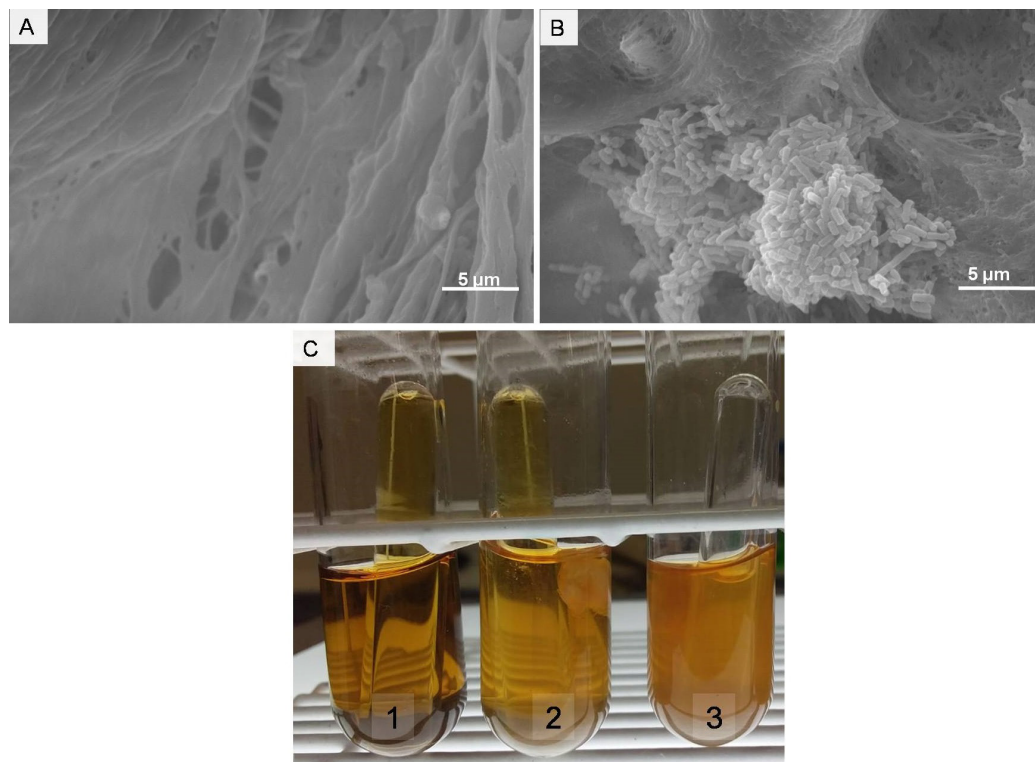


**Figure 8.** Microbial proliferation in PVA matrices and cell activity in lactose broth. The images shows foam with absence (a) and presence of bacteria *E.coli* (b) and (c) Durham tube assay: tube 1 – blank; tube 2- foam alone; tube 3- foam + microorganism.

capacity for proliferation and metabolism, however, further research is necessary to determine the performance of PVA matrix against different types of microorganisms regarding adhesion and metabolic activities profile.

#### 4. Conclusion

The use of gas foaming technique in combination with a controlled freeze-drying process led to the formation of highly porous PVA with characteristics suitable for microorganism 3D cell culture. The morphological, physicochemical, thermal and mechanical characterization confirmed that the PVA was cross-linked with glutaraldehyde. The analysis showed that thermal chemical and mechanical stability were improved after the PVA crosslinking. The morphological properties, swelling and degradation behavior in aqueous environment suggest that the PVA matrix has proper characteristics for 3D microorganism culture. *Escherichia coli* (Gram-negative bacteria), *Staphylococcus aureus* (Gram-positive bacteria) and *Candida albicans* (yeast) cells could adhere to the PVA matrix. In particular, *E. coli* adheres to biomaterial and this immobilization preserves the proliferative capacity of bacteria and the metabolic activity after 24 hours.

#### 5. Acknowledgments

The authors wish to thank the Brazilian National Council for the Improvement of Higher Education (CAPES) and the Minas Gerais Research Foundation (FAPEMIG) for financial support.

#### 6. References

1. Singh BK. Exploring microbial diversity for biotechnology: the way forward. Trends Biotechnol. 2010;28(3):111-6.
2. Tortora GJ, Case CL, Funke BR. Micro Biologia. Porto Alegre: ARTMED; 2017. 935 p.
3. Edmondson R, Broglie JJ, Adcock AF, Yang L. Three-dimensional cell culture systems and their applications in drug discovery and cell-based biosensors. Assay Drug Dev Technol. 2014;12(4):207-18.
4. Crabbé A, Liu Y, Matthijs N, Rigole P, De La Fuente-Núñez C, Davis R, et al. Antimicrobial efficacy against *Pseudomonas aeruginosa* biofilm formation in a three-dimensional lung epithelial model and the influence of fetal bovine serum. Sci Rep. 2017;7(March):1-13.
5. Ning E, Turnbull G, Clarke J, Picard F, Riches P, Vendrell M, et al. 3D bioprinting of mature bacterial biofilms for antimicrobial resistance drug testing. Biofabrication. 2019;11(4)
6. Bahamondez-Canas TF, Heersema LA, Smyth HDC. Current status of in vitro models and assays for susceptibility testing for wound biofilm infections. Biomedicine. 2019;7(2):1-31.
7. Lee J, Cuddihy MJ, Kotov NA. Three-dimensional cell culture matrices: state of the art. Tissue Eng Part B Rev. 2008;14(1):61-86.
8. Cai T, Chen L, Ren Q, Cai S, Zhang J. The biodegradation pathway of triethylamine and its biodegradation by immobilized *Arthrobacter protophormiae* cells. J Hazard Mater. 2011;186(1):59-66.
9. Liu H, Guo L, Liao S, Wang G. Reutilization of immobilized fungus *Rhizopus sp.* LG04 to reduce toxic chromate. J Appl Microbiol. 2012;112(4):651-9.
10. Devi S, Sridhar P. Production of cephamycin C in repeated batch operations from immobilized *Streptomyces clavuligerus*. Process Biochem. 2000;36(3):225-31.
11. Seung HS, Suk SC, Park K, Yoo YJ. Novel hybrid immobilization of microorganisms and its applications to biological denitrification. Enzyme Microb Technol. 2005;37(6):567-73.

12. Maltman DJ, Przyborski SA. Developments in three-dimensional cell culture technology aimed at improving the accuracy of *in vitro* analyses. *Biochem Soc Trans*. 2010;38(4):1072-5.
13. Okazaki M, Hamada T, Fujii H, Kusudo O, Mizobe A, Matsuzawa S. Development of poly(vinyl alcohol) hydrogel for waste water cleaning. II. Treatment of N,N-dimethylformamide in waste water with poly(vinyl alcohol) gel with immobilized microorganisms. *J Appl Polym Sci*. 1995;58(12):2243-9.
14. Martins SCS, Martins CM, Fiuza LMCG, Santaella ST. Immobilization of microbial cells: A promising tool for treatment of toxic pollutants in industrial wastewater. *Afr J Biotechnol*. 2013;12(28):4412-8.
15. Bezbradica D, Obradovic B, Leskosek-Cukalovic I, Bugarski B, Nedovic V. Immobilization of yeast cells in PVA particles for beer fermentation. *Process Biochem*. 2007;42(9):1348-51.
16. De Ory I, Romero LE, Cantero D. Optimization of immobilization conditions for vinegar production. Siran, wood chips and polyurethane foam as carriers for *Acetobacter aceti*. *Process Biochem*. 2004;39(5):547-55.
17. Bai X, Zheng-Fang Y, Yan-Feng L, Li-Cheng Z, Liu-Qing Y. Preparation of crosslinked macroporous PVA foam carrier for immobilization of microorganisms. *Process Biochem*. 2010;45(1):60-6.
18. O'Toole G, Kaplan HB, Kolter R. Biofilm formation as microbial development. *Annu Rev Microbiol*. 2000;54(1):49-79.
19. Ravi M, Paramesh V, Kaviya SR, Anuradha E, Paul Solomon FD. 3D cell culture systems: advantages and applications. *J Cell Physiol*. 2015;230(1):16-26.
20. Werthén M, Henriksson L, Jensen PØ, Sternberg C, Givskov M, Bjarnsholt T. An *in vitro* model of bacterial infections in wounds and other soft tissues. *APMIS*. 2010;118(2):156-64.
21. Martineau L, Dosch HM. *In vitro* bactericidal efficacy of a new sun- and heat burn gel. *Burns*. 2006;32(6):748-54.
22. Percival SL, Bowler PG, Dolman J. Antimicrobial activity of silver-containing dressings on wound microorganisms using an *in vitro* biofilm model. *Int Wound J*. 2007;4(2):186-91.
23. Wolcott RD, Rumbaugh KP, James G, Schultz G, Phillips P, Yang Q, et al. Biofilm maturity studies indicate sharp debridement opens a time-dependent therapeutic window. *J Wound Care*. 2010;19(8):320-8.
24. Woods J, Boegli L, Kirker KR, Agostinho AM, Durch AM, deLancey Pulcini E, et al. Development and application of a polymicrobial, *in vitro*, wound biofilm model. *J Appl Microbiol*. 2012;112(5):998-1006.
25. Ferreira FV, Souza LP, Martins TMM, Lopes JH, Mattos BD, Mariano M, et al. Nanocellulose/bioactive glass cryogels as scaffolds for bone regeneration. *Nanoscale*. 2019;11(42):19842-9.
26. Townsend EM, Sherry L, Rajendran R, Hansom D, Butcher J, Mackay WG, et al. Development and characterisation of a novel three-dimensional inter-kingdom wound biofilm model. *Biofouling*. 2016;32(10):1259-70.
27. Grassi L, Batoni G, Ostyn L, Rigole P, Van Den Bossche S, Rinaldi AC, et al. The antimicrobial peptide lin-SB056-1 and its dendrimeric derivative prevent pseudomonas aeruginosabiofilm formation in physiologically relevant models of chronic infections. *Front Microbiol*. 2019;10(Feb):1-14.
28. Choi SM, Singh D, Kumar A, Oh TH, Cho YW, Han SS. Porous three-dimensional PVA/gelatin sponge for skin tissue engineering. *Int J Polym Mater Polym Biomater*. 2013;62(7):384-9.
29. Loh QL, Choong C. Three-dimensional scaffolds for tissue engineering applications: role of porosity and pore size. *Tissue Eng Part B Rev*. 2013;19(6):485-502.
30. Eltom A, Zhong G, Muhammad A. Scaffold techniques and designs in tissue engineering functions and purposes: a review. *Adv Mater Sci Eng*. 2019; 2019:1-13.
31. Deville S. Ice-templating, freeze casting: beyond materials processing. *J Mater Res*. 2013;28(17):2202-19.
32. Figueiredo KCS, Alves TLM, Borges CP. Poly(vinyl alcohol) films crosslinked by Glutaraldehyde under mild conditions. *J Appl Polym Sci*. 2009;111:3074-80.
33. Zhang H, Zhou L, Zhang W. Control of scaffold degradation in tissue engineering: A review. *Tissue Eng Part B Rev*. 2014;20(5):492-502.
34. Göpferich A. Mechanisms of polymer degradation and erosion I. *Biomater Silver Jubil Compend*. 1996;17(2):117-28.
35. Peppas NA, Merrill EW. Differential scanning calorimetry of crystallized PVA hydrogels. *J Appl Polym Sci*. 1976;20(6):1457-65.
36. Dattola E, Parrotta EI, Scalise S, Perozziello G, Limongi T, Candeloro P, et al. Development of 3D PVA scaffolds for cardiac tissue engineering and cell screening applications. *RSC Advances*. 2019;9(8):4246-57.
37. Leblon CE, Pai R, Fodor CR, Golding AS, Coulter JP, Jedlicka SS. *In vitro* comparative biodegradation analysis of salt-leached porous polymer scaffolds. *J Appl Polym Sci*. 2013;128(5):2701-12.
38. Matta N, Bisht GRS. Detection and enumeration of coliforms in Ganga Water Collected from different ghats. *J Bioprocess Biotech*. 2018;8(2)
39. Mansur HS, Sadahira CM, Souza AN, Mansur AAP. FTIR spectroscopy characterization of poly (vinyl alcohol) hydrogel with different hydrolysis degree and chemically crosslinked with glutaraldehyde. *Mater Sci Eng C*. 2008;28(4):539-48.
40. Esparza Y, Ullah A, Boluk Y, Wu J. Preparation and characterization of thermally crosslinked poly(vinyl alcohol)/feather keratin nanofiber scaffolds. *Mater Des*. 2017;133:1-9.
41. Ricciardi R, Auriemma F, Gaillet C, De Rosa C, Lauprêtre F. Investigation of the crystallinity of freeze/thaw poly(vinyl alcohol) hydrogels by different techniques. *Macromolecules*. 2004;37(25):9510-6.
42. Gu ZQ, Xiao JM, Zhang X. The development of artificial articular cartilage – PVA-hydrogel. *Biomed Mater Eng*. 1998;8(2):75-81.
43. Nakaoki T, Yamashita H. Bound states of water in poly(vinyl alcohol) hydrogel prepared by repeated freezing and melting method. *J Mol Struct*. 2008;875(1-3):282-7.
44. Ma W, Zhang P, Zhao B, Wang S, Zhong J, Cao Z, et al. Swelling resistance and mechanical performance of physical crosslink-based Poly(Vinyl Alcohol) hydrogel film with various molecular weight. *J Polym Sci, B, Polym Phys*. 2019;57(24):1673-83.
45. Costa HS, Mansur AAP, Pereira MM, Mansur HS. Engineered hybrid scaffolds of poly(vinyl alcohol)/bioactive glass for potential bone engineering applications: Synthesis, characterization, cytocompatibility, and degradation. *J Nanomater*. 2012;2012(23)
46. Ye M, Mohanty P, Ghosh G. Morphology and properties of poly vinyl alcohol (PVA) scaffolds: impact of process variables. *Mater Sci Eng C*. 2014;42:289-94.
47. Tian H, Yuan L, Wang J, Wu H, Wang H, Xiang A, et al. Electrospinning of polyvinyl alcohol into crosslinked nanofibers: an approach to fabricate functional adsorbent for heavy metals. *J Hazard Mater*. 2019;378(February):120751.
48. Chen J, Li Y, Zhang Y, Zhu Y. Preparation and characterization of graphene oxide reinforced PVA film with boric acid as crosslinker. *J Appl Polym Sci*. 2015;132(22):1-8.
49. Watler PK, Cholakis CH, Sefton MV. Water content and compression modulus of some heparin-PVA hydrogels. *Biomaterials*. 1988;9(2):150-4.
50. Fan H, Hartshorn C, Buchheit T, Tallant D, Assink R, Simpson R, et al. Modulus-density scaling behaviour and framework architecture of nanoporous self-assembled silicas. *Nat Mater*. 2007;6(6):418-23.
51. Park SA, Lee SJ, Seok JM, Lee JH, Kim WD, Kwon IK. Fabrication of 3D Printed PCL/PEG polyblend scaffold using rapid prototyping system for bone tissue engineering application. *J Bionics Eng*. 2018;15(3):435-42.

52. Kim DH, Kim KL, Chun HH, Kim TW, Park HC, Yoon SY. In vitro biodegradable and mechanical performance of biphasic calcium phosphate porous scaffolds with unidirectional macro-pore structure. *Ceram Int.* 2014;40(6):8293-300.
53. Kim TR, Kim MS, Goh TS, Lee JS, Kim YH, Yoon SY, et al. Evaluation of structural and mechanical properties of porous artificial bone scaffolds fabricated via advanced TBA-based freeze-gel casting technique. *Appl Sci (Basel).* 2019;9(9):1-17.
54. Woignier T, Reynes J, Hafidi Alaoui A, Beurroies I, Phalippou J. Different kinds of structure in aerogels: relationships with the mechanical properties. *J Non-Cryst Solids.* 1998;241(1):45-52.
55. Morandim-Giannetti AA, Rubio SR, Nogueira RF, Ortega FS, Magalhães O Jr, Schor P, et al. Characterization of PVA/ glutaraldehyde hydrogels obtained using Central Composite Rotatable Design (CCRD). *J Biomed Mater Res B Appl Biomater.* 2018;106(4):1558-66.
56. Galya T, Sedlařík V, Kuřitka I, Novotný R, Sedlaříková J, Sába P. Antibacterial poly(vinyl alcohol) film containing silver nanoparticles: preparation and characterization. *J Appl Polym Sci.* 2008;110(5):3178-85.
57. Khan MQ, Kharaghani D, Nishat N, Shahzad A, Hussain T, Khatri Z, et al. Preparation and characterizations of multifunctional PVA/ZnO nanofibers composite membranes for surgical gown application. *J Mater Res Technol [Internet].* 2019;8(1):1328-34.
58. Sasaki S, Omata S, Murakami T, Nagasawa N, Taguchi M, Suzuki A. Effect of Gamma Ray Irradiation on Friction Property of Poly(vinyl alcohol) Cast-Drying on Freeze-Thawed Hybrid Gel. *Gels [Internet].* 2018;4(2):30.
59. Oh JK, Yegin Y, Yang F, Zhang M, Li J, Huang S, et al. The influence of surface chemistry on the kinetics and thermodynamics of bacterial adhesion. *Sci Rep.* 2018;8(1):1-13.
60. Maboni G, Davenport R, Sessford K, Baiker K, Jensen TK, Blanchard AM, et al. A novel 3D skin explant model to study anaerobic bacterial infection. *Front Cell Infect Microbiol.* 2017;7(Sep):1-12.
61. Heo I, Dutta D, Schaefer DA, Iakobachvili N, Artegiani B, Sachs N, et al. Modelling Cryptosporidium infection in human small intestinal and lung organoids. *Nat Microbiol.* 2018;3(7):814-23.
62. Leung JM, Rould MA, Konradt C, Hunter CA, Ward GE. Disruption of TgPHIL1 alters specific parameters of *Toxoplasma gondii* motility measured in a quantitative, three-dimensional live motility assay. *PLoS One.* 2014;9(1):1-10.
63. Kanatani S, Uhlén P, Barragan A. Infection by *Toxoplasma gondii* induces amoeboid-like migration of dendritic cells in a three-dimensional collagen matrix. *PLoS One.* 2015;10(9):1-16.
64. Danielson JJ, Perez N, Romano JD, Coppens I. Modelling *Toxoplasma gondii* infection in a 3D cell culture system In Vitro: comparison with infection in 2D cell monolayers. *PLoS One.* 2018;13(12):1-13.
65. Zaharia DC, Muntean AA, Popa MG, Steriade AT, Balint O, Micut R, et al. Comparative analysis of *Staphylococcus aureus* and *Escherichia coli* microcalorimetric growth. *BMC Microbiol.* 2013;13(1):1.
66. Gutiérrez MC, García-Carvajal ZY, Jobbágy M, Yuste L, Rojo F, Abrusci C, et al. Hydrogel scaffolds with immobilized bacteria for 3D cultures. *Chem Mater.* 2007;19(8):1968-73.